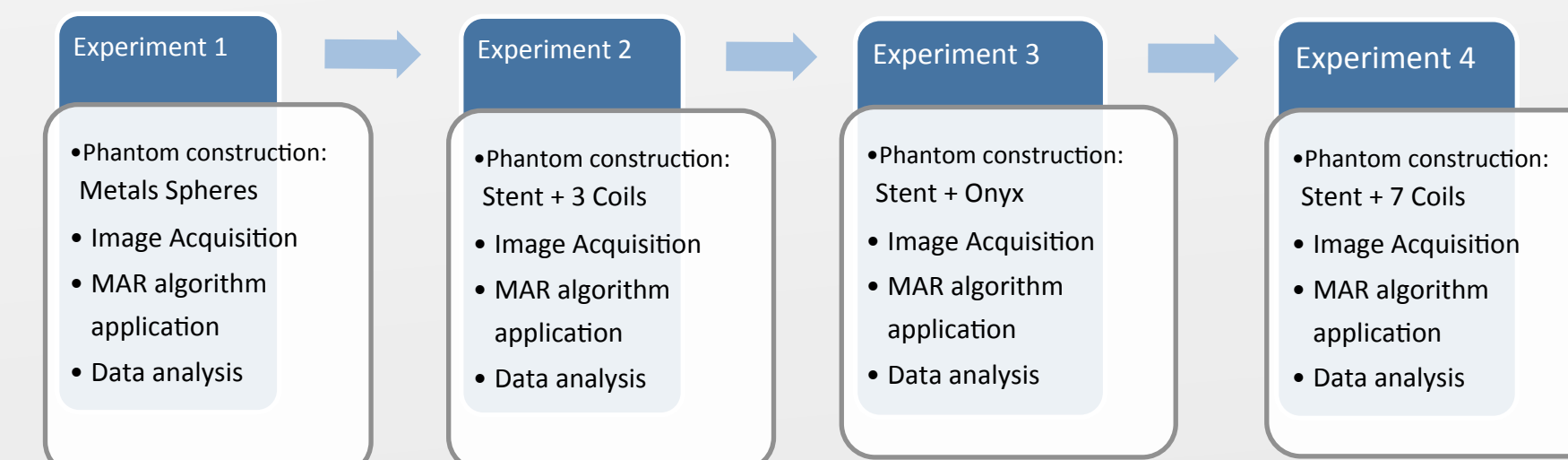


Introduction

- C-Arm CT guidance of neurovascular interventions for treatment of intracranial aneurysms is hindered by the presence of streak artifacts caused by metal implants.
- The purpose of this project was to design pre-clinical studies that would quantitatively evaluate the performance of a metal artifact reduction (MAR) algorithm.
- Optimizing and quantifying image quality will facilitate a safer, more accurate use of CT imaging in the surgical environment.



Problem and Solution

- C-Arm CT guided endovascular treatments for intracranial aneurysms include: stent-assisted endovascular coiling, surgical clipping and liquid embolization.



Figure 1. (a) stent-assisted coiling, (b) clipping, and (c) liquid embolization. Image by M. Headworth.

- Metal artifacts are caused by beam hardening (a shift in detected mean energy) and photon starvation (insufficient photons reach the detector). MAR algorithms that diminish these artifacts have been developed, but need to be thoroughly tested before clinical use.

- Four phantoms that emulate the abovementioned endovascular interventions were imaged using a Cone-Beam CT system. Data analysis was performed in uncorrected and MAR corrected data in order to identify algorithm components that require further improvements.

Methods

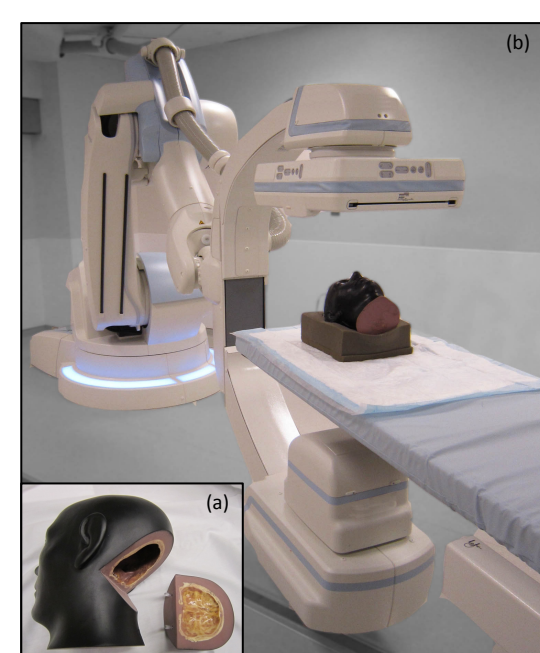


Figure 2. Experimental setup; (a) hollow brain phantom and (b) Siemens C-arm Cone-beam CT. Image provided by I-star lab.

- The brain phantom used consisted of a natural human skull with an opening at the base.
- The intracranial space was successfully filled with brain-equivalent gelatin, relevant low-contrast tissue plastics, prototype aneurysm vasculature trees and metal components.
- All scans were performed on a C-Arm Cone-Beam CT system (Siemens Healthcare).

Results

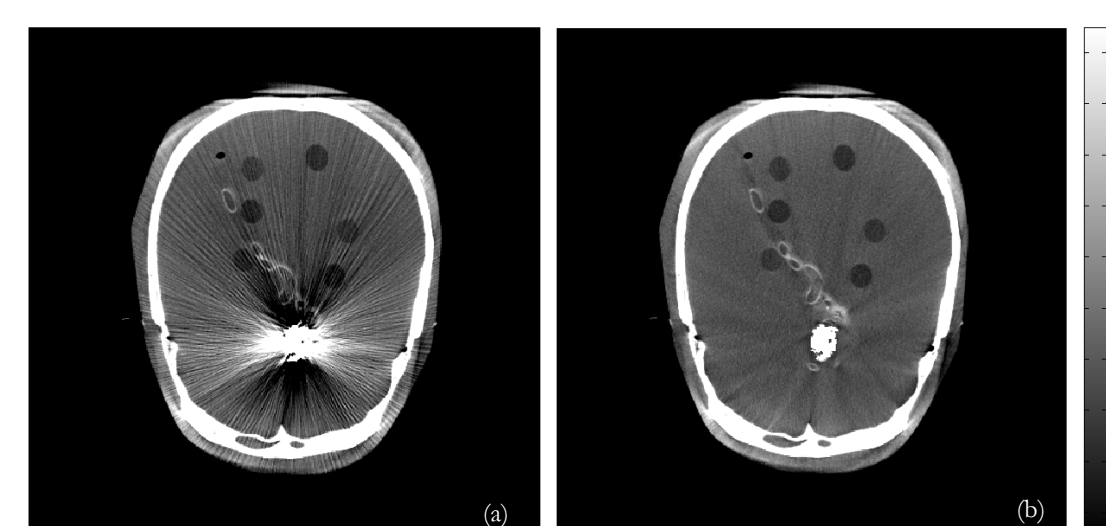


Figure 3. Head Phantom
(a) Uncorrected and (b) MAR corrected Cone-Beam CT images of brain phantom containing a coil-packed aneurysm.

METAL SPHERES PHANTOM MODEL:

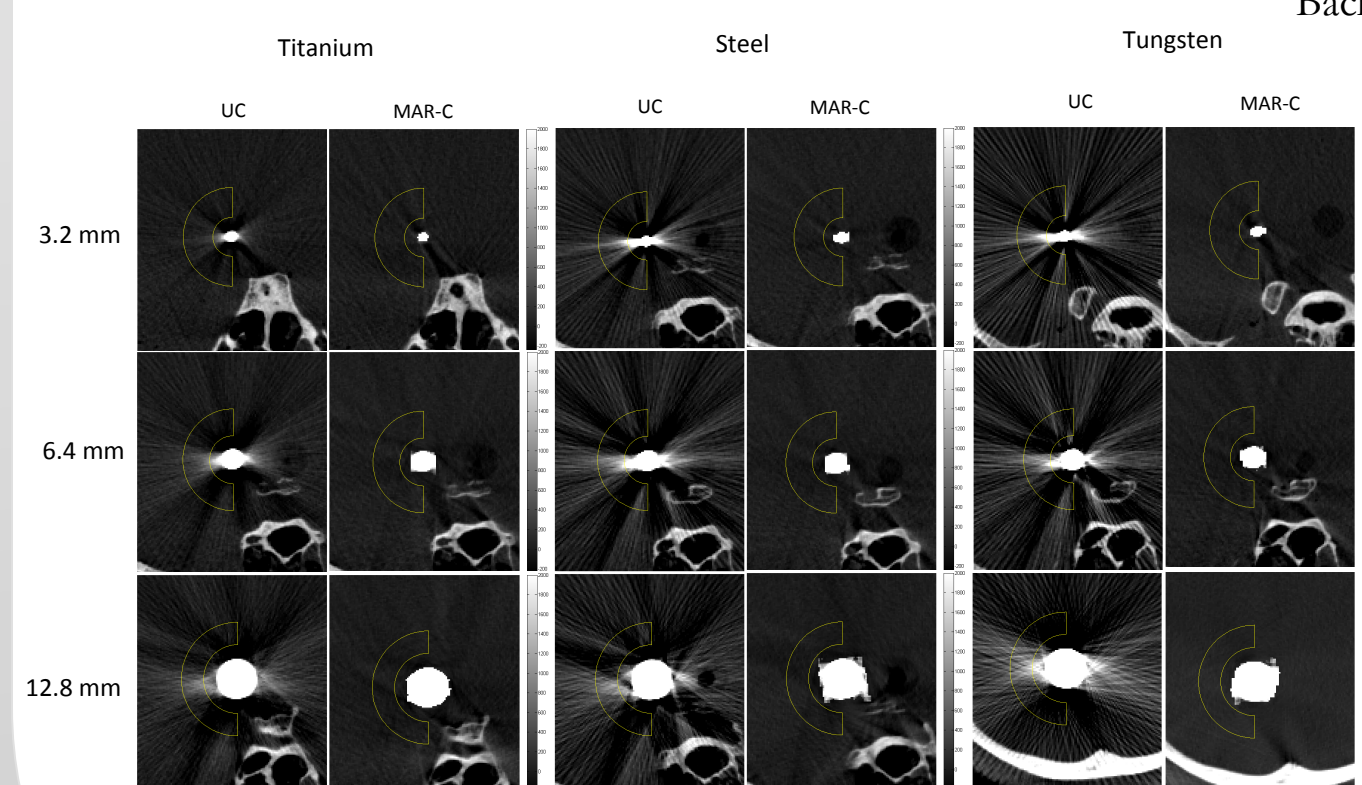


Figure 4. Zoomed-in uncorrected (UC) and MAR corrected (MAR-C) CT images of metal spheres of varying densities and diameters. Background ROIs are highlighted in yellow.

LIQUID EMBOLUS PHANTOM MODEL:

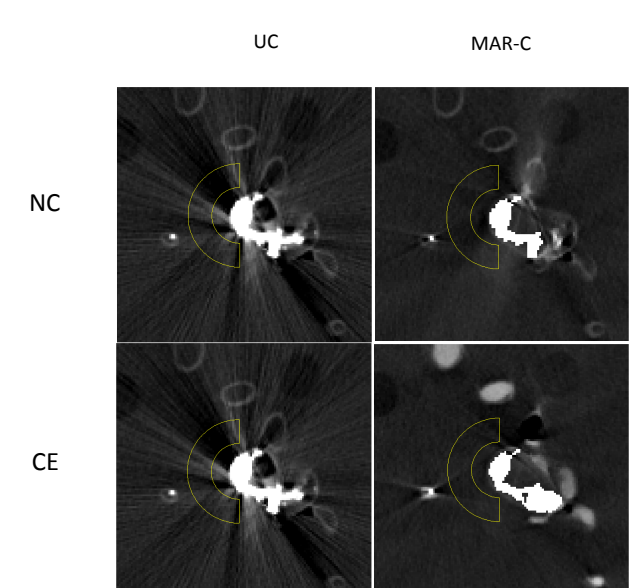


Figure 5. Zoomed-in uncorrected (UC) and MAR corrected (MAR-C) CT images of a liquid embolization (Onyx) in non-enhanced (NC) and contrast enhanced (CE) vessels. Background ROIs are highlighted in yellow.

STENT-ASSISTED COILING PHANTOM MODEL:

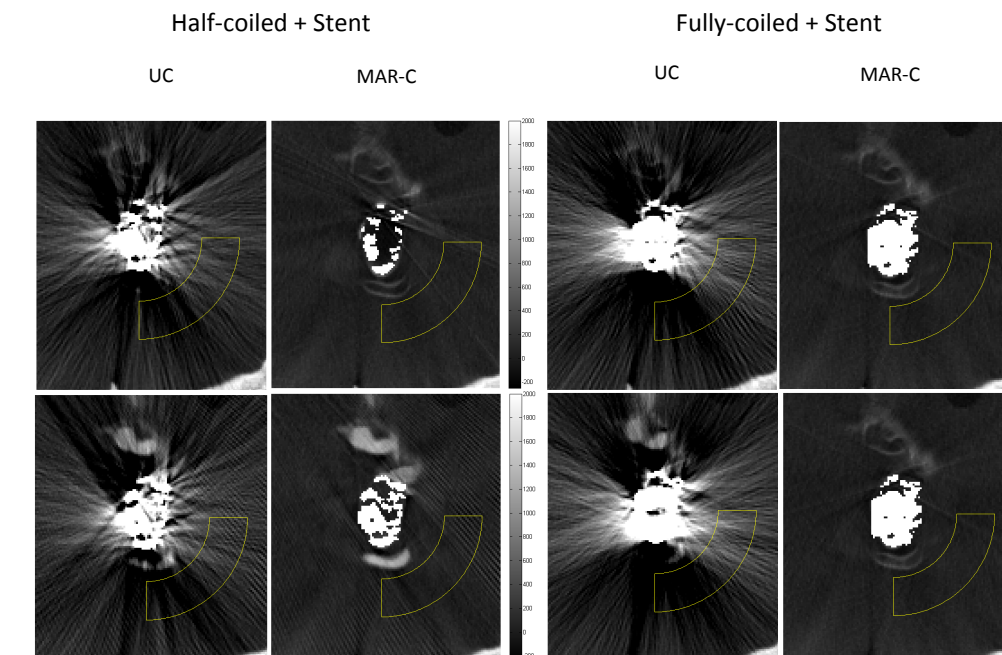
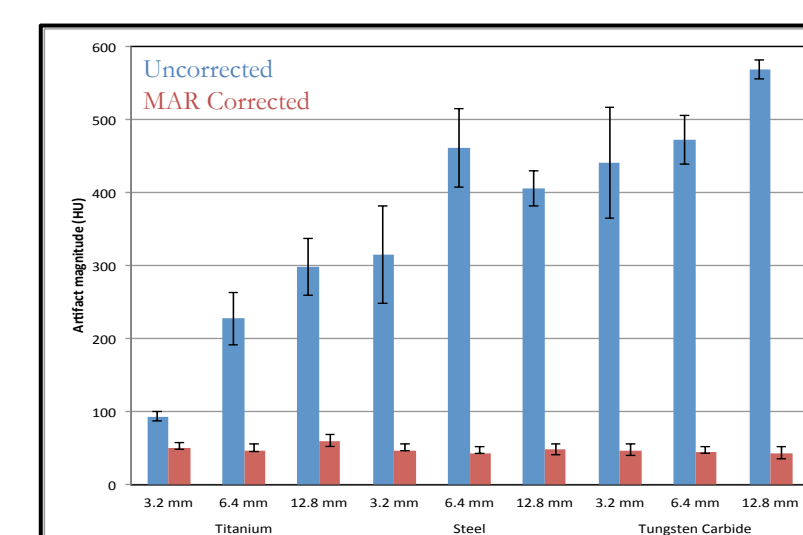
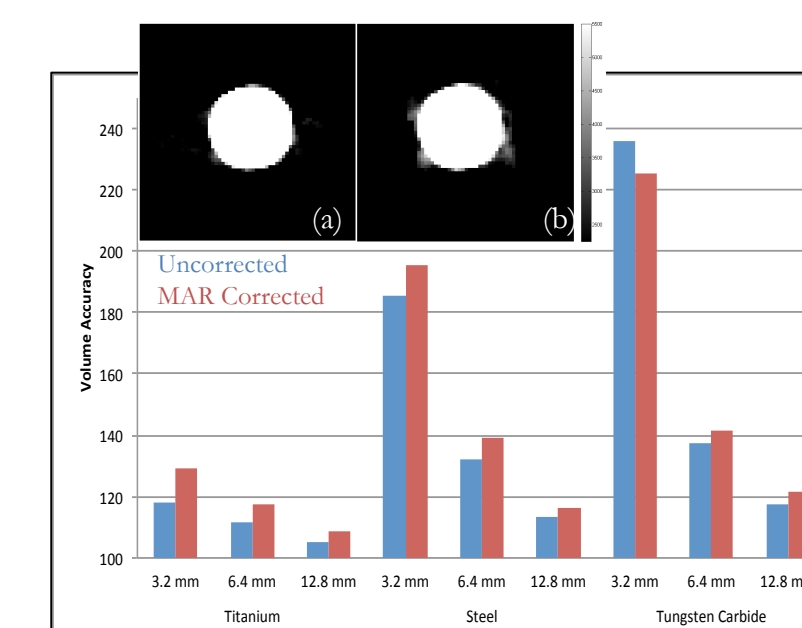


Figure 6. Zoomed-in uncorrected (UC) and MAR corrected (MAR-C) CT images of a stent-assisted aneurysm coiling in non-enhanced (NC) and contrast enhanced (CE) vessels. Background ROIs are highlighted in yellow.



Graph 1. Artifact magnitude of uncorrected and MAR corrected CT data of metal spheres. Artifact magnitude in uncorrected data is directly proportional to the density and diameter of the metal sphere. Notice that the MAR algorithm corrects the artifact magnitude to a constant level, regardless of density or diameter.



Graph 2. Volume accuracy of uncorrected and MAR corrected CT data of metal spheres. Lower volume accuracy indicates closer estimation of true volume values. MAR algorithm overestimates volume of metal component. Zoomed-in 12.8mm steel sphere (a) uncorrected and (b) MAR corrected in limited-window display.

- CT images were reconstructed with and without a MAR prototype developed by the manufacturer. Below is a flowchart of the MAR algorithmic steps.



- Image quality (degree of distortion introduced into the image) assessment includes: measurements of contrast, noise and artifact magnitude. Image fidelity (degree to which the image successfully represents the anatomy) assessments include: volumetric measurements of metal segmentation and the accurate representation of surrounding low-contrast tissue.

Measurement	Unit	Symbol/Equation
Mean	HU	$\mu_{\text{component} \& \text{background}}$
Artifact magnitude	HU	$\sigma_{\text{background}}$
CNR		$\frac{\mu_{\text{component}} - \mu_{\text{background}}}{\sigma_{\text{background}}}$
CT number error	%	$\left \frac{\mu_{\text{true}} - \mu_{\text{measured}}}{\mu_{\text{true}}} \right \cdot 100$
Sphericity		$\psi = \frac{\pi^{1/3} (6V)^{2/3}}{A_c}$
Volume accuracy	%	$\left \frac{V_{\text{measured}}}{V_{\text{true}}} \right \cdot 100$

Conclusions

- The MAR algorithm provided excellent reduction of artifact magnitude even for large and various metal components, but resulted in a slight distortion of the segmented shape of the metal inserts.
- This quantitative performance assessment indicates that the MAR method warrants investigation in clinical studies.

What's next?

Future work includes streamlining the semi-automatic segmentation step, analysis of tolerance to MAR parameters, and comparison to other MAR and segmentation approaches (e.g. Known-Component Reconstruction [Stayman, et al.]

What did we learn?

Image visualization is vital in CT-guided interventions. Quantifying image quality is important for: evaluating new imaging technology and algorithms; evidence for translation to clinical use; avoiding pitfalls of subjective interpretation.

Resources and Acknowledgments

- Thanks to Adam Wang for his help in the phantom construction and image acquisition, C. Rohkohl and B. Scholz for their work in development of the MAR algorithm & The Johns Hopkins Hospital, Siemens Healthcare, The I-STAR Lab, and ERC-CISST for the use of equipment and facilities.

Credits:

- Carolina Cay: in charge of project management and write-ups.
- Marta Wells: in charge of MATLAB coding of data analysis.
- Project members were equally involved in phantom construction and image acquisition in simulated neurovascular interventions.

[1] Barrett, J. F., and N. Keat. "Artifacts in CT: Recognition and Avoidance." Radiographics 24.6 (2004): 1679-691. Print.
 [2] Prell, D., Y. Kyriakou, T. Struffert, M. Beister, and W. A. Kalender. "A novel forward-projection based metal artifact reduction method for flat-detector computed tomography." Physics in Medicine and Biology 54 (2009): 6575-91. Print.
 [3] Stayman KCR, IEEE-TMI
 Abstract submitted to RSNA 99th annual conference